

Exploiting Perceptual Anchoring for Color Image Enhancement

減少背光耗電, & keep Image 色彩

Kuang-Tsu Shih and Homer H. Chen, *Fellow, IEEE*

Abstract—The preservation of image quality under various display conditions becomes more and more important in the multimedia era. A considerable amount of effort has been devoted to compensating the quality degradation caused by dim LCD backlight for mobile devices and desktop monitors. However, most previous enhancement methods for backlight-scaled images only consider the luminance component and overlook the impact of color appearance on image quality. In this paper, we propose a fast and elegant method that exploits the anchoring property of human visual system to preserve the color appearance of backlight-scaled images as much as possible. Our approach is distinguished from previous ones in many aspects. First, it has a sound theoretical basis. Second, it takes the luminance and chrominance components into account in an integral manner. Third, it has low complexity and can process 720p high-definition videos at 35 frames per second without flicker. The superior performance of the proposed method is verified through psychophysical tests.

Index Terms—Anchoring theory, color appearance model, color image enhancement, human perception.

I. INTRODUCTION

MOST multimedia devices are equipped with a panel display today [1], [2]. This is unlikely to change in the foreseeable future. The panel display usually consumes a significant portion of the energy of a multimedia device. For example, among all components, the backlight module of a liquid crystal display (LCD) may consume as much as 50% of the total power for a smartphone in the video playing mode [3]. This is a major concern for most mobile devices because of limited battery capacity. Reducing the power of the backlight module is an effective means to save energy and extend the battery life. However, dim backlight severely degrades the quality of image luminance and chrominance. As shown in Fig. 1(a), when the backlight is switched to a low power level, the color and detail of the woods region in the image can hardly be seen. To further

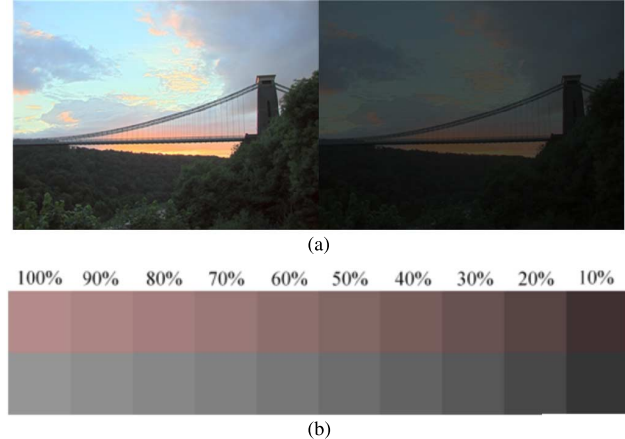


Fig. 1. Demonstration of the effect of backlight-scaling on image appearance. All backlight-scaled images in this figure are generated by the procedure described in Section V-B. (a) The original image (left) and its backlight-scaled image (right). (b) Color patches illuminated with backlight of different intensities. The backlight-scaling ratios are shown at the top of each column.

耗電：且降低背光會 degraded 亮度 + 色度
illustrate the chrominance degradation, two patches illuminated with various backlight intensities are shown in Fig. 1(b), where the pink block and the achromatic gray block are set at the same luminance level. We can see that the two patches become less distinguishable as the backlight goes dimmer.

The importance of the need for compensating the undesirable effect of dim backlight cannot be overstated for mobile devices nowadays [4], [5]. The issue can be broadly described as that of color image enhancement across different reproduction conditions, whether the backlight-scaled image is displayed on the same LCD or not. The issue exists in many other multimedia applications as well. For example, in high dynamic range (HDR) image tone mapping, the luminance of a scene spanning nearly ten orders has to be reproduced on a display with merely three orders of dynamic range [6]. Another example is ubiquitous projection, where a projector has to overcome the effects of color and texture of a non-white projection surface so that the image would appear as if it were projected on a white screen [7], [8]. Likewise, in energy-aware video streaming where the multimedia clients often work in a low-backlight condition to save energy, the server has to take the effect of dim backlight on the display into consideration to achieve high quality of experience on the client side [9], [10].

The image is ultimately watched by a human. Therefore, properties of the human visual system (HVS) have to be taken into consideration for image enhancement. Because color perception is a psychological process, preserving color sensation across different image reproduction conditions is often more

HVS 是依照定錯特性(anchor)來感知 color

Manuscript received April 22, 2015; revised September 08, 2015 and November 04, 2015; accepted November 18, 2015. Date of publication November 25, 2015; date of current version January 15, 2016. This work was supported in part by the National Science Council of Taiwan under Contract NSC 100-2221-E-002-197-MY3, in part by the National Taiwan University under Contract NTU-CESRP-102R7609-2, and in part by Himax Technologies, Inc. under Contract 101-S-C37. The associate editor coordinating the review of this manuscript and approving it for publication was Dr. Wolfgang Hurst.

K.-T. Shih is with the Graduate Institute of Communication Engineering, National Taiwan University, Taipei 10617, Taiwan (e-mail: shihkt@gmail.com).

H. H. Chen is with the Department of Electrical Engineering, Graduate Institute of Communication Engineering and the Graduate Institute of Networking and Multimedia, National Taiwan University, Taipei 10617, Taiwan (e-mail: homer@ntu.edu.tw).

Color versions of one or more of the figures in this paper are available online at <http://ieeexplore.ieee.org>.

Digital Object Identifier 10.1109/TMM.2015.2503918

important than retaining the physical color. This is especially the case for the enhancement of backlight-scaled images considered in this work, for which the image luminance cannot be recovered unless the backlight power is returned to the full level. 利用 HVS 的 anchor 特性，在降低背光時，增強 color image

Most previous methods for backlight-scaled image enhancement [11]–[14] either overlook the impact of color appearance on image quality or separately consider the processing of luminance and chrominance, leading to improper or mismatched chrominance adjustment.

The study of HVS suggests that our brain processes a color stimulus relative to an anchor (a reference value) corresponding to the display condition [15]. Our color sensation of a stimulus is maintained under a different display condition if the stimulus relative to the anchor is preserved. In this paper, this property of human visual perception is exploited for backlight-scaled image enhancement. Our approach allows the compensation of the undesired effects of dim backlight in an integral manner. It has a sound theoretical basis—the anchoring property of HVS—and enhances the color appearance of images in a way that matches human perception. Furthermore, it works consistently well for different images and avoids unnatural color appearance caused by the mismatch between luminance and chrominance components. The low computational complexity of this approach is attractive for energy-aware multimedia applications [16]–[19].

This paper distinguishes from its conference version [20] in three aspects. First, a post gamut mapping algorithm is developed to better preserve the image details. Second, new experiments are conducted to compare the proposed method with existing methods. Lastly, a discussion on the impact of the color appearance model on the overall system performance is provided. 低 complexity 算法，避免亮色不匹配出的不自然 color

II. RELATED WORK

In this section, we give an overview of perceptual models for human color perception and methods for enhancing image appearance.

A. Color Appearance Models 匹配人類感知色彩的量化 module (3個)

To accurately preserve the color sensation across various display conditions, a precise quantification of color appearance that matches human perception is required. This subject has been studied for long in color science. Many color models with emphasis on the effect of viewing condition have been developed recently.

1. X: RG
2: B Y: 亮度

An early model called XYZ quantifies color sensation through a strictly controlled matching experiment [21]. It has two disadvantages. First, it is not perceptually uniform. In other words, the Euclidean distance between two points in the XYZ space does not correlate well with the perceptual difference between the color stimuli represented by the points. Second, it works only if the viewing condition in the original experiment is satisfied.

To improve perceptual uniformity, color opponent spaces such as CIELAB [22] were developed. Unlike the XYZ model, the three dimensions of a color opponent space have clear perceptual meaning: One represents lightness, one the red-green opponent color channel, and the other the yellow-blue opponent

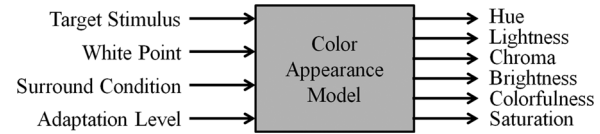


Fig. 2. Inputs and outputs of a typical color appearance model.

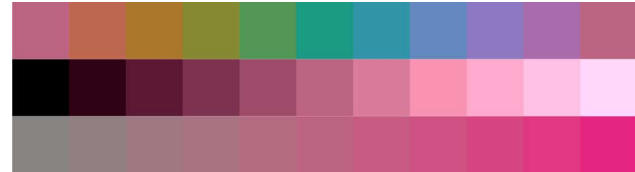


Fig. 3. Color patches having different hue values (top row), lightness values (middle row), and chroma values (bottom row). The value increases from left to right for lightness and chroma.

特性和模型	XYZ 模型	CIELAB 模型	CIECAM02 模型
维度	3 维 ($X - Y - Z$)	3 维 ($L^* - a^* - b^*$)	多维 (Hue, Lightness, Chroma 等)
数据空间	绝对空间	相对空间	非绝对空间
感知均匀性	低	中等	高
输入数据	三刺激值 ($X - Y - Z$)	三刺激值 ($X - Y - Z$) + 视觉条件参数	三刺激值 ($X - Y - Z$) + 视觉条件参数
输出数据	$X - Y - Z$	L^* (明度), a^* (红绿), b^* (黄蓝)	Hue (色调), Lightness (明度), Brightness (亮度), Chroma (饱和度), Colorfulness (色彩强度), Saturation (饱和度)
是否考虑视觉条件	否	否	是
需用颜色校正	基本色彩匹配	色彩差异计算、颜色校正、色彩增强	精确色彩重现、颜色校正、色彩增强
优点	能效、简单化	感知均匀性好, XYZ 好	高准确度、可逆性
缺点	非感知均匀性, 受观者视觉条件影响	未考虑视觉条件	被接受度较低
应用限制	基本色彩匹配	色彩差异计算、印像、基本影像处理	高精度色彩重现、HDR、显示校正、影像增强

color channel. Although such a color appearance model is more perceptually uniform than the XYZ model, the viewing condition is not taken into account.

A color appearance model can be categorized according to the viewing condition on color perception. Most of the models of modeling many color appearance attributes can be modeled by the XYZ space. The typical inputs and outputs of a color appearance model are shown in Fig. 2. The input is the target color stimulus along with a set of parameters describing the viewing condition. The outputs are the predictors of the color appearance attributes: hue, lightness, brightness, chroma, colorfulness, and saturation. Fig. 3 shows color patches that differ in hue, lightness, and chroma. These attributes can be classified into two categories: absolute and relative. The difference between them is subtle but important (see Section III).

There are many color appearance models developed for various applications [22]–[26]. Among them, CIECAM02 [27] is recommended for general color reproduction due to its accuracy and simple reversibility [15].

B. Gamut Mapping 色域 mapping

Gamut mapping is the operation of assigning a point in the target gamut to a corresponding point in the source gamut. It is usually incorporated in color reproduction systems [28], [29]. Existing gamut mapping algorithms (GMAs) can be classified into two categories: reduction and expansion. Reduction GMAs are designed for the scenario where the volume of the target gamut is smaller than that of the source gamut, whereas expansion GMAs are designed for the scenario where the volume of the target gamut is larger than that of the source gamut. Current research on gamut mapping falls mostly into the first category, so does this work because the target low-backlight gamut is much smaller than the source full-backlight gamut.

Reduction algorithms can be further categorized into two types according to their mapping strategy. One type adopts the clipping strategy [30] and only acts on the points outside the target gamut while leaving the other in-gamut point intact. In contrast, the other type adopts the compression strategy [31]–[34] and remaps every point in the source gamut no matter whether the point is in the target gamut or not. For this type of

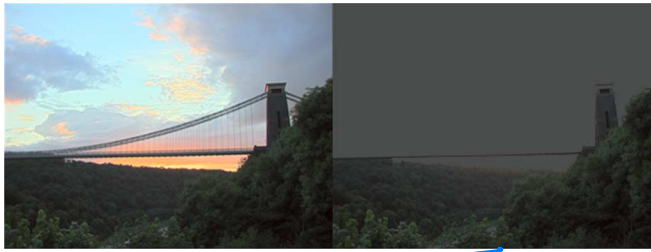


Fig. 4. GMA with the clipping strategy wipes out image details in bright regions. The left is the original image and the right is the gamut-mapped image.

GMA and hue simultaneously map source gamuts to target ones. It may result in loss of pixels, which is unnecessary. The target gamut and target gamuts may fail others. Although a general-purpose GMA is desired, no satisfactory solution has been found yet. In addition, there is no consensus about the state-of-the-art GMA due to the lack of a good evaluation method [28].

C. Enhancement Methods for Backlight-Scaled Images

Existing enhancement methods for backlight-scaled images can be classified into two categories. The first category aims at preserving the luminance contrast between the bright regions of the backlight and the dark regions of the image. The second category targets enhancing the visual quality of the image under dim backlight [12]–[14].

To preserve the luminance of each pixel, methods in the first category determine the lowest possible dimming ratio (usually no lower than 50%) on the fly according to the image content. Targeting primarily at energy saving, these methods usually require the local intensity of the backlight to be controllable.

On the other hand, methods in the second category can be applied to images illuminated by backlight with a very low dimming ratio (as low as 10%). The typical procedure of such methods is shown in Fig. 5. The luminance layer is first extracted (either in HSV space [14] or YCbCr space [12], [13]) from the input image and then decomposed into a detail layer (high-passed) and a base layer (low-passed). Such decomposition is implemented through a convolution with a spatially invariant low-pass kernel [12], an adaptive nonlinear filtering scheme based on the just noticeable difference (JND) [13], or a minimization of the total variation of the base layer [14]. The two layers are then processed independently and combined with the chrominance layer of the input image to generate the enhanced result. Typically, the compression of luminance is performed only on the base layer to preserve local contrast as much as possible, while the detail layer is either untouched [12], [13] or passed to a contrast enhancement scheme [14]. In contrast to the delicate processing of the luminance layer, the chrominance layer is left untouched by most existing methods.

現有的背光縮減影像增強方法可分為兩大類：

• 保留像素亮度的方法 [35, 36] :

◦ 這類方法旨在不同背光功率等級下保留像素的亮度。

◦ 根據影像內容，來決定最低可能的背光調光比率（通常不低於 50%）。

◦ 主要目標：節能省電。

◦ 要求：通常需要能夠局部控制背光強度。

• 提升低照光動態可見度的方法 [12]–[14] :

◦ 適用於在非光紙的背光比率下（低至 10%）照相的影像。

◦ 應該方法的典型處理流程如圖 5 所示。

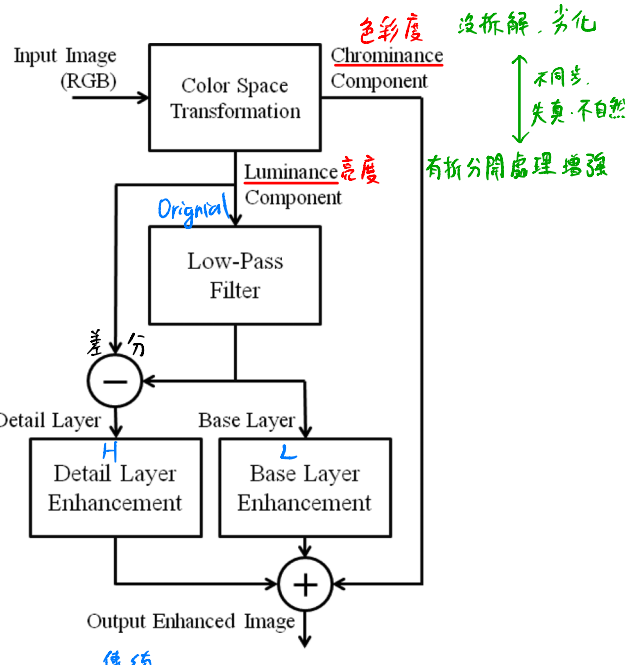


Fig. 5. Flowchart of conventional backlight-scaled image enhancement.



Fig. 6. Conventional backlight-scaled image enhancement algorithms fail to preserve the contrast between the woods and the sky. The left is the original image and the right is the result of Pei [10].

One main drawback of such methods is that the *global* contrast may not be preserved in the enhanced image. As shown in Fig. 6, the luminance contrast between the bright region (sky) and the dark region (woods) in the original image is destroyed in the enhanced image. In addition, such methods only work on the luminance layer and pay little attention to the chrominance degradation.

D. Display Characterization

Display characterization is important for accurate color reproduction. It aims at characterizing the relation between input RGB values and output XYZ values of displays. The relation is usually expressed by a mathematical function (the display model) with a set of parameters. $\text{output: } XYZ \Rightarrow \text{input: } RGB$

A typical procedure of display characterization goes as follows. First, a display model is determined for the target display. Note that, in this step, only the form of the mathematical model is determined and the parameters are not yet known. Next, a sample set containing multiple color samples is picked, and the XYZ values of the color samples are measured using a colorimeter. The number of color samples increases with the number of parameters of the display model. Finally, the obtained groundtruth XYZ values are used to estimate the parameters of

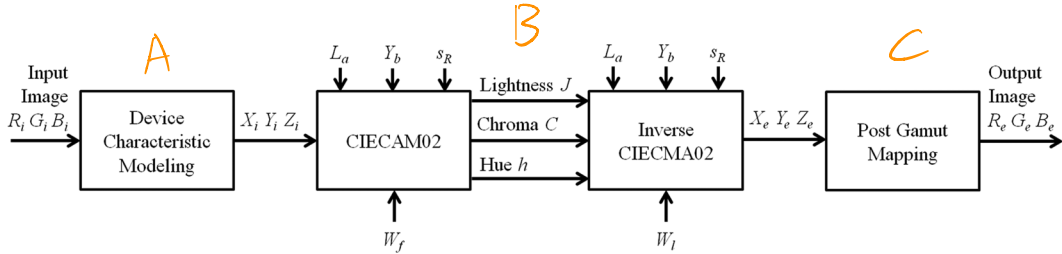


Fig. 7. Flowchart of the proposed algorithm. The white points for the forward and the inverse models are set different.

function, Ex.

the display model by I
tained, the XYZ value

There are many dis
various displays [37].
(GOG) model [38] ta
and the S-curve model
developed for LCDs.

顯示器特性化模型示例

1. GOG 模型 (Gain-Offset-Gamma Model) [38] :
 - 適用範圍：陰極射線管 (CRT) 顯示器。
 - 特點：考慮了效益 (Gain)、偏移 (Offset) 和伽瑪 (Gamma) 訂正。
2. S 曲線模型 (S-Curve Model) [39] :
 - 適用範圍：液晶顯示器 (LCD)。
 - 特點：模擬 LCD 的非線性輸出特性。
3. 多項式模型 (Polynomial Model) [40] :
 - 適用範圍：液晶顯示器 (LCD)。
 - 特點：使用多項式函數來擬合顯示器的色彩輸出特性，適合複雜的顯示器行為。

III. THE ANCHORING PROPERTY

運用定锚特性進行影像增強技術的核心在於：
• 透過調整亮度和對比度，讓人類視覺系統在低背光條件下感知到更高的亮度，
 以此來強調色彩的真實感。這段文字將會進一步闡述 HVS 的定锚特性。

It is widely accepted that HVS functions more than a light sensor. To illustrate this point, consider a piece of paper at night and a lamp under sunlight. Although physically the latter emits more light than the former, we still perceive the former to be brighter. This common experience suggests that HVS judges color appearance in a relative manner by comparing the physical color of a stimulus with the anchor determined by the viewing condition. Because the anchor at night is much darker than that in daytime, the paper is perceived brighter than the lamp. Similarly, for an LCD, when the backlight intensity is lowered, the HVS tends to overestimate the light emitted by the display, resulting in a higher perceptual response. The overestimation is, again, the result of a darker anchor corresponding to the low-backlight display.

This important property of the HVS has been incorporated into color appearance models. As described in Section II-A, a color appearance model generates both absolute and relative perceptual attributes. Relative attributes are used to describe visual sensations that involve a comparison with the anchor, whereas the absolute attributes are used to describe sensations that are independent of the anchor. Although in some situations (e.g. observing a light source in a dark room) the absolute attributes are more meaningful than the relative attributes, the relative perception often plays a more important role in our daily visual experiences.

IV. THE PROPOSED ENHANCEMENT ALGORITHM

To cope with the anchoring property of human color perception, our enhancement algorithm preserves the relative attributes (lightness, hue, and chroma) across different backlight intensities. The flowchart of the proposed enhancement algorithm is shown in Fig. 7. It has three main steps, namely, display characterization, color reproduction, and post gamut mapping. We describe them in detail in this section.

① gamma 線性化
② Matrix \Rightarrow XYZ

Since our enhancement algorithm targets faithful color reproduction, high-precision characterization is necessary. For that, we adopt the following display model:

$$\begin{bmatrix} X \\ Y \\ Z \end{bmatrix} = \mathbf{M} \begin{bmatrix} R_l \\ G_l \\ B_l \end{bmatrix} = \begin{bmatrix} m_{rx} & m_{gx} & m_{bx} \\ m_{ry} & m_{gy} & m_{by} \\ m_{rz} & m_{gz} & m_{bz} \end{bmatrix} \begin{bmatrix} R^{\gamma_r} \\ G^{\gamma_g} \\ B^{\gamma_b} \end{bmatrix} \quad (1)$$

where γ_r , γ_g , and γ_b , respectively, denote the gamma values of the red, green, and blue channels, (R, G, B) denotes the normalized device-dependent pixel value in the input image, (R_l, G_l, B_l) denotes the linear RGB value, and (X, Y, Z) denotes the resulting XYZ tristimulus value. (1) transfers the input pixel value from the device-dependent RGB space to the device-independent XYZ color space.

There are a total of 12 model parameters (three gamma values and nine transformation matrix entries) in (1) that need to be determined. Define the following sample values:

解 3+9
define $\left\{ \begin{array}{l} C_R = \left\{ \left(\frac{15 + 16k}{255}, 0, 0 \right) | k = 0, 1, 2, \dots, 15 \right\} \\ C_G = \left\{ \left(0, \frac{15 + 16k}{255}, 0 \right) | k = 0, 1, 2, \dots, 15 \right\} \\ C_B = \left\{ \left(0, 0, \frac{15 + 16k}{255} \right) | k = 0, 1, 2, \dots, 15 \right\} \end{array} \right. \quad (2)$

這些 sample
 $16 \times 4 - 4 + 1 = 61$ Samples
and \Rightarrow 色度計量 61 sample 的 $\begin{bmatrix} X \\ Y \\ Z \end{bmatrix}$ 值，估算出 Matrix + gamma (12)

$$C_A = \left\{ \left(\frac{15 + 16k}{255}, \frac{15 + 16k}{255}, \frac{15 + 16k}{255} \right) | k = 0, 1, 2, \dots, 15 \right\}. \quad (3)$$

$$C_A = \left\{ \left(\frac{15 + 16k}{255}, \frac{15 + 16k}{255}, \frac{15 + 16k}{255} \right) | k = 0, 1, 2, \dots, 15 \right\}. \quad (4)$$

\Rightarrow Table I

C_R contains red samples, C_G green samples, C_B blue samples, and C_A achromatic samples. These samples (a total of 60) plus the RGB value $(0, 0, 0)$ form a sample color set. After the ground truth of the 61 sample colors in the XYZ space is obtained using a colorimeter, the 12 model parameters are estimated by convex optimization.

The characterization is performed for the full-backlight display and the low-backlight display. The resulting estimated gammas are denoted by $\gamma_{r,f}$, $\gamma_{g,f}$, and $\gamma_{b,f}$ for the full-backlight display and $\gamma_{r,l}$, $\gamma_{g,l}$, and $\gamma_{b,l}$ for the low-backlight display. Likewise, the resulting transformation matrices for the full-backlight and the low-backlight displays are denoted by \mathbf{M}_f and \mathbf{M}_l , respectively. The parameter estimation does not need to be performed for each new image. The same parameters can be used till the display is recalibrated.

The XYZ tristimulus value (X_i, Y_i, Z_i) of an arbitrary pixel in the original image is obtained from the RGB value



Fig. 8. Original image (left) and the out-of-gamut pixels (right), where pixels whose red channel is not in the $[0, 1]$ range are marked red. Similarly, the green and blue out-of-gamut pixels are marked in the right image.

(R_i, G_i, B_i) by substituting $(R, G, B) = (R_i, G_i, B_i)$, $\gamma_r = \gamma_{r,f}$, $\gamma_g = \gamma_{g,f}$, $\gamma_b = \gamma_{b,f}$, and $\mathbf{M} = \mathbf{M}_f$ into (1).

B. Color Reproduction

We seek to preserve the relative attributes of lightness, chroma, and hue using a color appearance model. Such appearance reproduction has been known since the early 1990s and is adopted in our algorithm. In this step, the point of the highest luminance in the display gamut is selected to be the anchor. This way, the anchor is only determined by the dimming ratio, which is independent of the input image. Among the existing color appearance models, we adopt CIECAM02 in this work for its accuracy and the simplicity of the inverse operation [41]. The entire set of equations in CIECAM02 can be found in [27]. For convenience, the input-output relationship of CIECAM02 is denoted by $\psi(\cdot)$. The inputs are the XYZ tristimulus value of the target, the luminance of the adaptation field, the luminance of the background field, and the surround condition. The outputs are the six attributes of color perception.

In this step, we first compute the XYZ value of the anchor for the full-backlight display W_f by setting $R = G = B = 1$, $(\gamma_r, \gamma_g, \gamma_b) = (\gamma_{r,f}, \gamma_{g,f}, \gamma_{b,f})$, and $\mathbf{M} = \mathbf{M}_f$ in (1). Similarly, we obtain the anchor for the low-backlight display W_l by setting $R = G = B = 1$, $(\gamma_r, \gamma_g, \gamma_b) = (\gamma_{r,l}, \gamma_{g,l}, \gamma_{b,l})$, and $\mathbf{M} = \mathbf{M}_l$ in (1). Next, we obtain the relative attributes (lightness J , chroma C , and hue h) from the color appearance model

$$\text{if } < \frac{\text{full}}{\text{low}} \quad (J, C, h) = \psi(X_i, Y_i, Z_i, W_f, L_a, Y_b, s_R) \quad (6)$$

where L_a is the absolute adapting luminance measured in cd/m^2 , Y_b is the relative luminance of the background, and s_R is the surround parameter. The enhanced XYZ value is obtained from the inverse color appearance model $\psi^{-1}(\cdot)$ by

$$\text{if } < \frac{\text{full}}{\text{low}} \quad (X_e, Y_e, Z_e) = \psi^{-1}(J, C, h, W_l, L_a, Y_b, s_R). \quad (7)$$

Note that the low-backlight anchor W_l serves as the white point in the inverse color appearance model.

C. Post Gamut Mapping

The enhanced XYZ value (X_e, Y_e, Z_e) may fall outside the low-backlight gamut for some pixels. A sample image of out-of-gamut pixels is shown in Fig. 8. We see that there are still a few bright and highly-saturated pixels that are outside the low-backlight gamut. These out-of-gamut pixels have to be brought back in the display gamut. To do this, we adopt a soft clipping GMA here to avoid introducing unnecessary distortion to the in-gamut pixels, which are the majority.

TABLE I
ESTIMATED DISPLAY PARAMETERS

Parameter*	Value	Parameter*	Value
$\gamma_{r,f}$	2.4767	$\gamma_{r,l}$	2.2212
$\gamma_{g,f}$	2.4286	$\gamma_{g,l}$	2.1044
$\gamma_{b,f}$	2.3792	$\gamma_{b,l}$	2.1835
\mathbf{M}_f	$\begin{bmatrix} 95.57 & 64.67 & 33.01 \\ 49.49 & 137.29 & 14.76 \\ 0.44 & 27.21 & 169.83 \end{bmatrix}$	\mathbf{M}_l	$\begin{bmatrix} 4.61 & 3.35 & 1.78 \\ 2.48 & 7.16 & 0.79 \\ 0.28 & 1.93 & 8.93 \end{bmatrix}$

*The symbols are defined in Section IV-A.

To alleviate the undesired loss of image details caused by clipping (discussed in Section VII-B), we adopt a weighted-average approach that outputs a linear combination of the clipped RGB value and the original RGB value for each pixel. Since both the clipped and the original RGB value are within the low-backlight gamut, their weighted average is guaranteed to be inside the gamut as well. Furthermore, through the selection of the weight, the output value of a pixel can be controlled towards the original pixel value or the clipped pixel value. Since brighter and more saturated colors suffer more from the clipping artifact, the weight for such pixels can be adjusted accordingly to preserve the image details.

In this step, a color transformation from the XYZ space to the RGB space is first applied to obtain the intermediate RGB value (R', G', B') for each pixel

$$\text{② linear } (R', G', B') = \left(R_{e,l}^{\frac{1}{\gamma_{r,l}}}, G_{e,l}^{\frac{1}{\gamma_{g,l}}}, B_{e,l}^{\frac{1}{\gamma_{b,l}}} \right) \quad (8)$$

where

$$\text{① } \begin{array}{c} \text{XYZ} \\ \Downarrow \\ \text{RGB} \end{array} \quad [R_{e,l} \ G_{e,l} \ B_{e,l}]^T = \mathbf{M}_l^{-1} [X_e \ Y_e \ Z_e]^T. \quad (9)$$

The clipped value (R_c, G_c, B_c) of a pixel is computed by

$$\text{③ clip } (R_c, G_c, B_c) = (f(R'), f(G'), f(B')) \quad (10)$$

where

$$\text{④ 限制在 } [0, 1] \quad f(x) = \begin{cases} x, & \text{if } 0 \leq x \leq 1 \\ 1, & \text{if } x > 1 \\ 0, & \text{if } x < 0. \end{cases} \quad (11)$$

Here, a pixel is out-of-gamut if its R' , G' , or B' is outside the range $[0, 1]$. The final enhanced RGB value (R_e, G_e, B_e) is obtained by linearly combining the clipped RGB value and the original RGB value

$$\text{⑤ } \begin{bmatrix} R_e \\ G_e \\ B_e \end{bmatrix} = (1 - JC) \begin{bmatrix} R_c \\ G_c \\ B_c \end{bmatrix} + JC \begin{bmatrix} R_i \\ G_i \\ B_i \end{bmatrix}. \quad (12)$$

We choose JC as the weight on (R_i, G_i, B_i) so that the enhanced RGB value of bright and saturated pixels are biased towards their original RGB value. Such bias reduces the loss of image details.

The proposed post gamut mapping algorithm has low computational complexity because it is performed in the RGB space (where the gamut is cube-shaped and hence the calculation of the gamut boundary is straightforward) instead of the XYZ

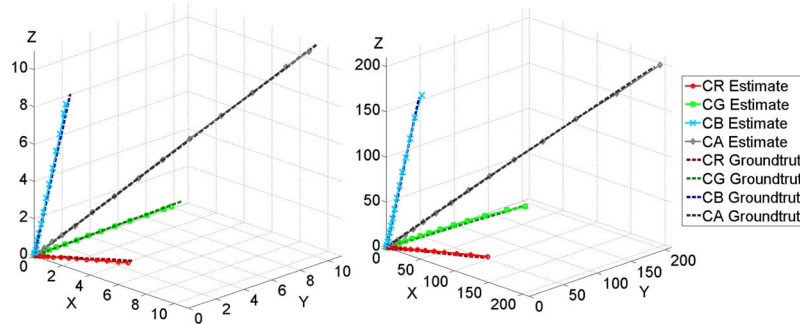


Fig. 9. The dashed-line curves connect the ground truth of the samples C_R , C_G , C_B , and C_A and the solid-line curves connect the estimated XYZ values of the samples. The left is the result for the low-backlight display and the right is the result for the full-backlight display.

space (where the gamut has non-planar boundary). In addition, parallel processing can be carried out to achieve further acceleration because of the spatial invariance property of the algorithm, where the computation involved in (8)–(12) for each pixel is independent of its neighbors.

V. EXPERIMENTAL RESULTS

The success of the proposed algorithm is hinged on the performance of display characterization. Two experiments are set up to evaluate the accuracy of display characterization and the quality of the enhanced images.

A. Performance Evaluation of Display Characterization

This experiment involves three steps: color sample measurement, display parameter estimation, and calculation of estimation error. In the first step, a Laiko DT-101 colorimeter is used to measure the XYZ value of every sample in C_R , C_G , C_B , and C_A defined in (2)–(5). In the second step, the measured values are used to estimate the display parameters (γ_r , γ_g , γ_b , M) according to the procedure described in Section IV-A. The estimated parameters are listed in Table I. In the third step, the estimation error is obtained by computing the average CIEDE2000 color difference between the ground truth and the estimated XYZ values. The average CIEDE difference is 2.60 for the full-backlight display and 2.65 for the low-backlight display.

The dashed curves in Fig. 9 connect the ground truth of the samples, and the solid curves connect the estimated XYZ values of the samples. We can see that the solid curves are in close proximity to their corresponding dashed curves in the XYZ space, indicating that the display model (1) and the estimated parameters together accurately characterize the displays.

B. Quality Evaluation of Enhanced Images

We apply the proposed algorithm to enhance uniform color patches and natural images illuminated with dim backlight in this experiment. The parameters of CIECAM02 are set as follows according to the viewing condition: The absolute luminance of the adapting field L_a is 63 (measured by a colorimeter), and the relative luminance of the background Y_b is 25 (one fourth of the relative luminance of the reference white). Since the experiments are performed in a well-illuminated lab, the surround condition is set to “average” according to Fairchild [15].

It should be pointed out that the results should be evaluated on an LCD rather than on a printout of the paper. Ideally, the

$$\left\{ \begin{array}{l} L_a = 63 \\ Y_b = 25 = \frac{1}{4} \cdot 100 \text{ (白:100)} \end{array} \right.$$

performance evaluation should be conducted on a pair of displays having the same characteristics. However, it is more convenient for us to evaluate the proposed method on simulated low-backlight displays. The display parameters are generated by the proposed method. For the simulated low-backlight, the display parameters are adjusted to illuminate the display with a low-backlight intensity (R_s, G_s, B_s) .

1. 符合低背光顯示特性
• 模擬低背光顯示效果：透過 $M_f^{-1} M_l$ 這個矩陣轉換，將增強後的 RGB 值 R_e, G_e, B_e 調整為低背光條件下的 RGB 值 (R_s, G_s, B_s) ，使得在全背光顯示器上顯示時，看起來像是在低背光顯示器上顯示的效果。

模擬所用的 RGB 值 (13)

$$(R_s, G_s, B_s) = \left(R_{s,l}^{\frac{1}{\gamma_r,f}}, G_{s,l}^{\frac{1}{\gamma_g,f}}, B_{s,l}^{\frac{1}{\gamma_b,f}} \right) \quad (13)$$

where

$$(2) \quad (R_s, G_s, B_s) = \left(R_{s,l}^{\frac{1}{\gamma_r,f}}, G_{s,l}^{\frac{1}{\gamma_g,f}}, B_{s,l}^{\frac{1}{\gamma_b,f}} \right) \quad (13)$$

 非線性化 low

$$(1) \quad \left[\begin{array}{l} R_{s,l} \\ G_{s,l} \\ B_{s,l} \end{array} \right] = M_f^{-1} M_l \left[\begin{array}{l} R_e^{\gamma_r,l} \\ G_e^{\gamma_g,l} \\ B_e^{\gamma_b,l} \end{array} \right]. \quad (14)$$

 在 full 的 LCD 上的 sim 線性化 low

For a thorough quality evaluation using two displays, the enhanced images are available on our website.¹

The experimental results for uniform color patches and natural images are shown in Figs. 10 and 11, respectively. For the ease of evaluation, we slightly increase the brightness of the resulting images. Specifically, these images are generated by (13) and (14) but with a different set of low-backlight display parameters obtained by characterizing the LCD with a higher backlight intensity. For the reader to have a feel of the actual brightness, we show in Fig. 12 one set of results that are generated with the original display parameters. The proposed method is compared against six existing methods: Pei [14], Huang [13], temporally aware backlight scaling (TABS) [11], adaptive backlight image enhancement (ABIE) [12], multi-scale retinex algorithm (Retinex) [9], and gamma correction (Gamma) with a fixed gamma value 0.5. In Fig. 10, uniform white patches are appended to indicate the backlight intensity.

From the results shown in Fig. 10, we can see that the color patches generated by the retinex algorithm, ABIE and TABS are too dark and do not resemble the original image, and that the chroma and hue of the gamma corrected results deviate seriously from the original patch. On the other hand, the lightness of the green patch in the first row produced by Pei is overly enhanced. This is more obvious if we compare the contrast between the green patch and the red patch in the second row before and after enhancement. Likewise, Huang tends to

¹“MPAC Lab,” [Online]. Available: <https://goo.gl/RTzqLq>

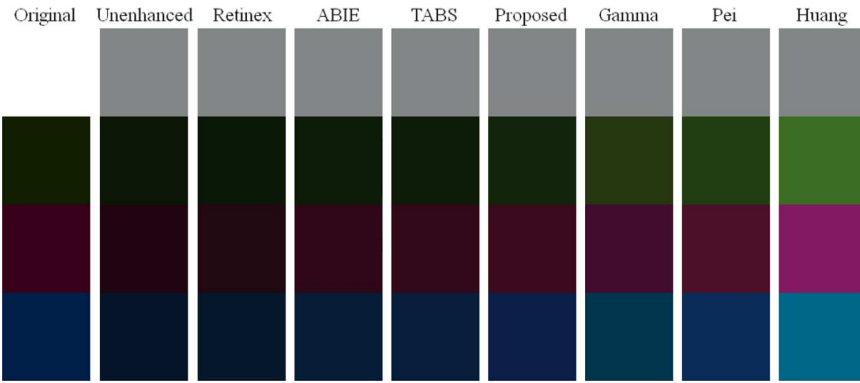


Fig. 10. Color enhancement performance comparison. The first column shows the original patches illuminated with full backlight, the second column shows the patches illuminated with dim backlight without enhancement, and the other columns show the enhanced patches produced by various methods.

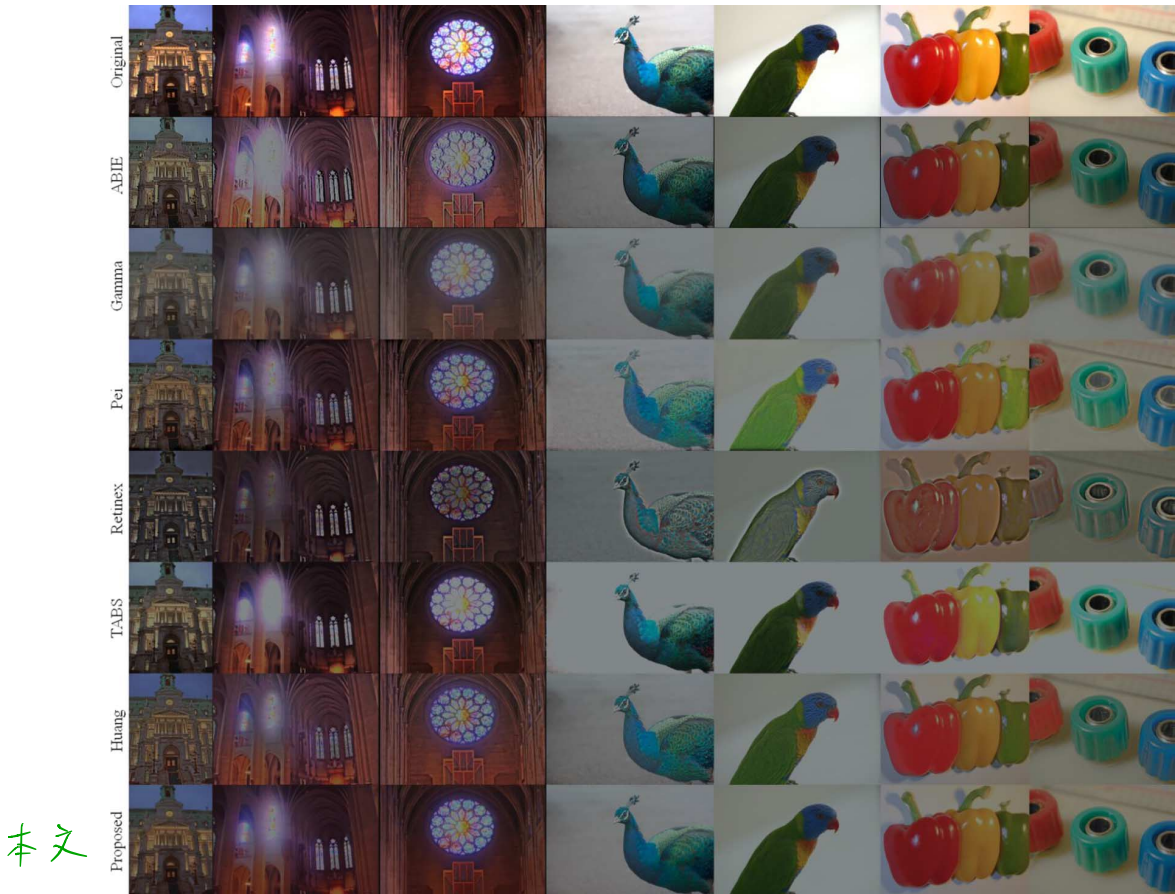


Fig. 11. Original images illuminated with full backlight and the enhanced images illuminated with dim backlight (simulated). Images in each row are generated by the same method, and the name of the method is shown on the left.

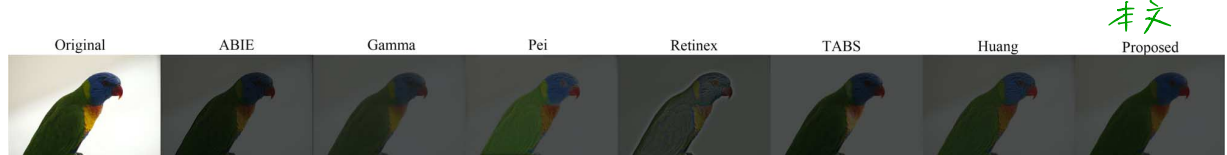


Fig. 12. Original image illuminated with full backlight and the enhanced images illuminated with dim backlight (simulated). The simulated backlight intensity is set equal to that of the real low-backlight display.

generate overly bright and saturated results. Because both Pei and Huang decompose an image based on the spatial frequency of the image, they may fail for uniform color patches, which have no high-frequency component.

From Fig. 11 we can see that ABIE and TABS fail to preserve details in the bright region of the image (e.g. the color glass windows, particularly the one with strong glare, in the second column and the third column), and that the chroma pro-

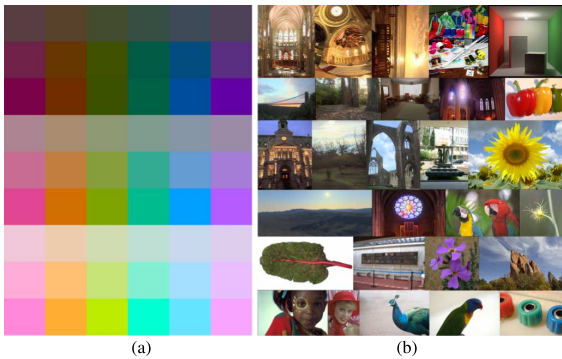


Fig. 13. (a) shows the 54 color patches and (b) shows the 28 natural images used in the psychophysical tests.

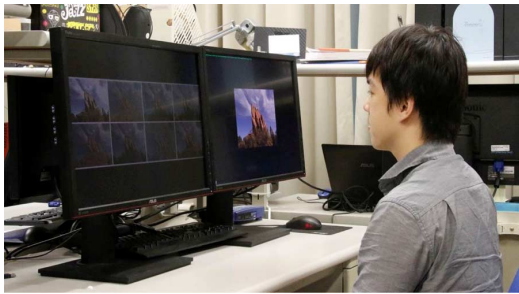


Fig. 14. Setup of the psychophysical tests. A low-backlight display and a full-backlight display are placed side by side in a well-illuminated lab.

duced by Gamma is so low that the images appear grayish although the lightness is effectively boosted. On the other hand, Pei over-boosts the dark regions (e.g. the parrot's body in the fifth column, the green pepper in the sixth column, and the dark hole of the center object in the seventh column). It can also be seen that Retinex produces undesirable ringing artifact due to low-pass filtering and that the resulting images appear grayish. Although Huang effectively enhances the details in the dark region, it sometimes fails to preserve the global contrast of the image. For example, the ceiling in the enhanced image in the second column appears almost as bright as the pillar on the right, but in fact it should be darker than the pillar.

VI. PSYCHOPHYSICAL TESTS

Two psychophysical tests were conducted to evaluate the performance of the proposed method. The 54 uniform color patches shown in Fig. 13(a) were used as test images in the first test, and the 28 natural images shown in Fig. 13(b) were used as test images in the second test. The uniform color patches were generated by the combination of three lightness levels, three chroma levels, and six hue values, whereas the set of natural images were selected such that it includes both indoor and outdoor scenes.

In both tests, two LCDs with the parameters specified in Table I were placed side by side in a well-illuminated lab. Two ViewSonic VG2427wm LCDs were used, one set to the full backlight level and the other to its lowest backlight level, as shown in Fig. 14. Each original image was displayed on the full-backlight LCD and the corresponding enhanced images produced by the methods described in Section V-B were displayed on the low-backlight LCD in random order. Twenty-six

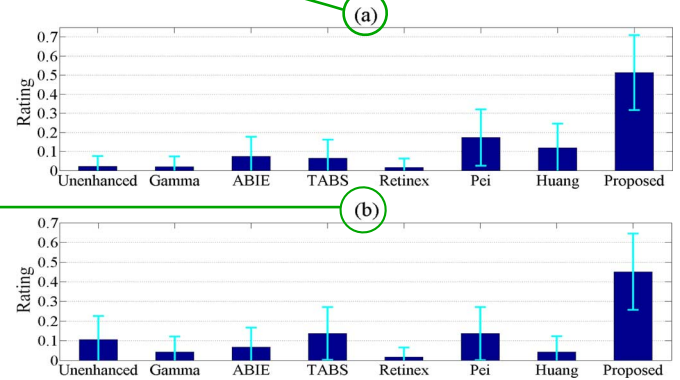


Fig. 15. Psychophysical test results for (a) color patches and (b) natural images. The horizontal axis represents different methods and the vertical axis is the probability that a method is rated best by subjects. The error bars represent the 95% confidence interval.

subjects with normal color vision were invited to participate in the tests and asked to choose from the enhanced images the one that appears closest to the original image. The viewing distance is approximately 50 cm, making the display extends approximately 63 degrees in the subject's field of view (FOV). Each color patch shown on the display extends approximately 8 degrees, and each natural image extends roughly 18 degrees in the subject's FOV. The images were shown with a black background to ensure that there is no brighter color stimulus within the central 63 degrees. The test room was set up such that no direct light source (e.g. lamp) or sun light appeared in the peripheral area beyond 63 degrees.

The results of the tests are shown in Fig. 15. For each method, we calculate the probability of being rated as the best by subjects. The error bars representing the 95% confidence interval are plotted to show the reliability of the results. We can see that the proposed method performs much better than the other methods.

VII. DISCUSSION

In this section, we discuss the impact of the color appearance model on the proposed color image enhancement method, the significance of the post gamut mapping developed along with the proposed method, and some useful applications of the proposed method.

A. Selection of Color Appearance Model

A. 色彩外觀模型的選擇
本研究採用了 CIECAM02 模型來計算相對的感知屬性（如明度 J 、色度 C 和色相 h ）。任何其他能夠預測這些屬性的可逆色彩外觀模型都可以納入該演算法中。為了研究色彩外觀模型對整體色彩影像增強性能的影響，我們將 CIECAM02 替換為三種其他色彩外觀模型：CIELAB [22]、RLAB [23] 和 Nayatani 模型 [24] [25]。Hunt 模型 [26] 未被考慮，因為它的反向模型無法以解析形式表達，精確度不如上述模型 [15]。

增強的色彩貼片和自然影像分別顯示在圖 16 和 圖 17 中。我們可以看到，CIELAB 模型無法很好地保留色度和明度，並且輸出仍然顯得暗淡且灰蒙蒙。另一方面，RLAB 模型有效提高了亮度，但會產生過度曝光的影像，並在亮區域中抹去了細節，如 圖 17 中第四行所示。此外，我們還可以看到 Nayatani 模型產生過度飽和的影像（例如， 圖 17 中第三列岩石影像的天空區域），這是因為它並非專為影像重現應用設計 [15]。

很明顯，在四種現有的色彩外觀模型中，CIECAM02 的表現最為穩健和令人滿意。

in Figs. 16 and 17, respectively. We can see that the CIELAB model does not preserve chroma and lightness very well and that

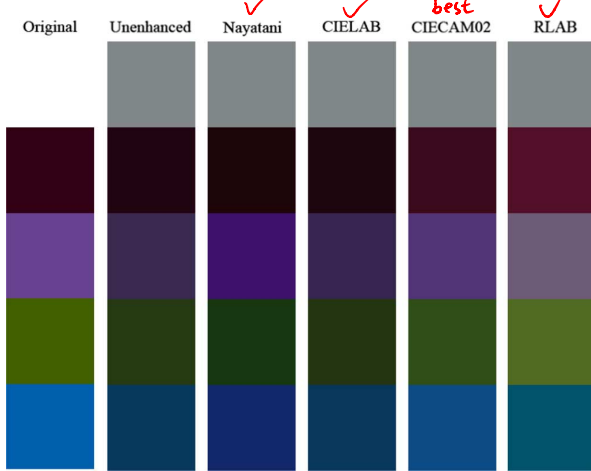


Fig. 16. Enhanced color patches generated by adopting various existing color appearance models in our algorithm. The name of the color appearance model used is shown at the top of each column.

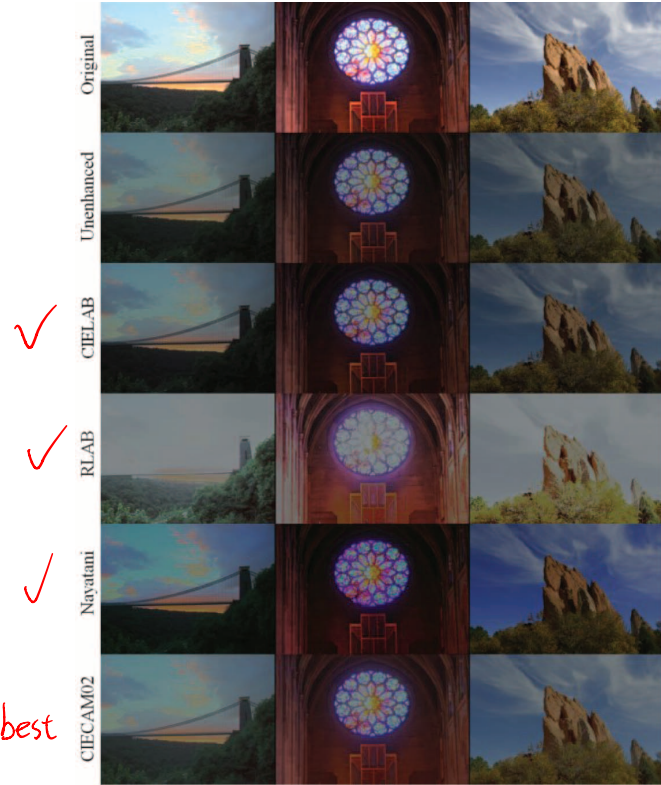


Fig. 17. Enhanced natural images generated by adopting various existing color appearance models in our algorithm. The name of the color appearance model is shown at the left of each row.

the output still appears dark and grayish. On the other hand, the RLAB model boosts the brightness effectively, but it produces overly exposed images and wipes out the details in bright regions as shown in the fourth row of Fig. 17. We can also see that the Nayatani model produces overly saturated images (see, for example, the sky region of the rock image in the third column of Fig. 17) because it is not originally designed for image reproduction applications [15].

It is clear that, among the four existing appearance models, CIECAM02 has the most robust and satisfactory performance.

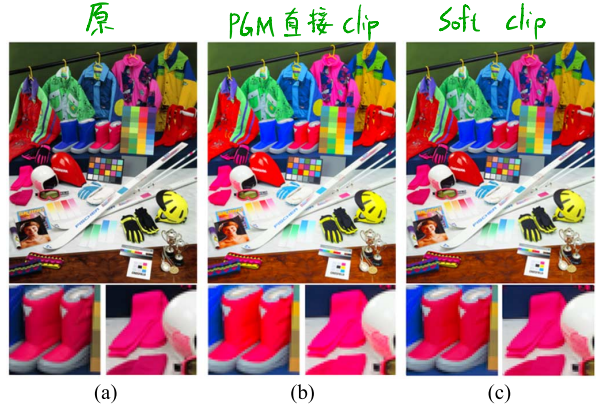


Fig. 18. Enhanced images generated by different gamut mapping strategies. (a) The original image. (b) The image generated by direct clipping. (c) The image generated by the proposed method. Selected close-ups of the enhanced images are shown in the second row.

TABLE II
COMPUTATION TIME OF THE PROPOSED METHOD

Input Image Size	1280x720	1920x1080
Number of Test Images	20	20
Average Computation Time (ms)	28.5	61.9
Standard Deviation (ms)	2.3	4.2

B. Effect of Post Gamut Mapping

B. 後色域映射的效果

在這裡，我們比較了由兩種不同的後色域映射策略生成的影像：所提出的方法和直接剪切 RGB 值的方法（公式 10）。

結果如圖 18 所示。我們可以看到，雖然由直接剪切方法生成的影像看起來比所提出的方法更亮且飽和度更高，但在高度飽和顏色的區域中，如靴子和圍巾的紋理，細節已經遺失，這可以從裁剪的特寫圖中看出。

相反，所提出的方法能有效保留這些區域的細節，同時不會犧牲低飽和度區域（如綠色背景）的色彩外觀。結果顯示，所提出的方法能重現原始影像的色彩外觀，同時保留影像的細節。

tively preserves the details in these regions without sacrificing the color appearance of less saturated regions such as the green background. The results show that the proposed method reproduces the color appearance of the original image and preserve the details of the image as well.

C. Computation Time

C. 計算時間

我們在 HD (1280×720) 影像和 Full HD (1920×1080) 影像上測試了我們方法的運算速度。我們的演算法在一臺運行 Windows 7 的桌面電腦上用 MATLAB 實現，該電腦配備 3.60GHz Intel Core i3-4160 處理器和 6GB 記憶體。

Table II 顯示了平均運算時間。我們可以看到，我們的程式每秒可處理 16 張 Full HD 影像和 35 張 HD 影像。這表示我們的方法能夠進行即時影片增強。

此外，由於我們的方法具有非自適應性和空間不變性，增強後的影像序列不會出現閃爍現象。enhanced sequence is free of flicker due to the non-adaptive and spatially invariant nature of our method.

D. Applications

D. 應用

我們的方法最初是為了薄膜電晶體液晶顯示器 (TFT-LCD) 的背光模組所開發，用於控制光源強度。然而，這種方法也可以應用於其他面板顯示器，因為所有面板顯示器，包括 OLED 和 AMOLED，都具備控制光源強度的機制，並且在光源強度較低時，都同樣需要進行影像色彩增強【43】。

這種方法的應用不僅限於儲存影像或影片的顯示，它還可以用於節能型影片串流服務【16】-【19】。在這些服務中，色彩增強的計算負擔可以放在伺服器端，而非用戶端，從而進一步節省能

耗。而，伺服器根據客戶端的需求，生成不同分辨率等級的影片。

除了用於背光調整影像增強外，我們的方法也可應用於反向色調映射【44】、【45】，這種技術用於擴展影像的動態範圍，使其適合 HDR 顯示器。反向色調映射的本質是根據不同的顯示條件，進行影像品質增強【46】。唯一的差別在於亮度基準的不同。在這個應用中，我們的方法可用於提升多媒體設備上 HDR 顯示器的影像色彩效果，以提供更好的觀賞體驗。

need for image color enhancement when the light intensity is low [43].

The application of the proposed method is not limited to the display of stored images or videos. It can be adopted in energy-aware video streaming services [16]–[19] where the computational load of color enhancement is placed on the server, instead of the clients, to achieve further energy saving. The server generates video at various energy-saving levels at the request of the clients.

In addition to the enhancement of backlight-scaled images, our method can also be applied to inverse tone mapping [44], [45] that expands the dynamic range of images for HDR displays and is essentially about the enhancement of image quality under a different display condition as well [46]. The only difference is the brightness of the anchor. In this application, our method can be applied to enhance the color appearance of images shown on multimedia devices with an HDR display to achieve better viewing experience.

VIII. CONCLUSION

VIII. 結論

在本文中，我們描述了一種針對低背光 LCD 顯示器下影像進行色彩外觀增強的方法。我們的方法能夠整合處理亮度與色度成分，從而避免亮度和色度調整之間可能出現的不匹配。此外，該方法足夠簡單，能夠實現即時的影片增強。心理物理測試表明，該方法有效提升了背光調整影像的視覺品質，並且表現優於現有的增強方法。

致謝

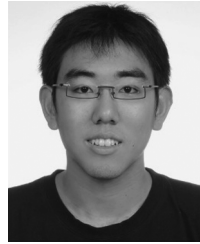
作者們感謝 S.-L. Yeh 教授 指出本文中所描述的核心思想在視覺科學中被稱為 人類視覺系統 (HVS) 的 鑑定特性 (anchoring property)。

The authors would like to thank Prof. S.-L. Yeh for pointing out that the main idea described in this paper is called the anchoring property of HVS in vision science.

REFERENCES

- [1] Y. Nimmagadda, K. Kumar, and Y.-H. Lu, “Adaptation of multimedia presentations for different display sizes in the presence of preferences and temporal constraints,” *IEEE Trans. Multimedia*, vol. 12, no. 7, pp. 650–664, Nov. 2010.
- [2] C. Deng, W. Lin, and J. Cai, “Content-based image compression for arbitrary-resolution display devices,” *IEEE Trans. Multimedia*, vol. 14, no. 4, pp. 1127–1139, Aug. 2012.
- [3] A. Carroll and G. Heiser, “An analysis of power consumption in a smartphone,” in *Proc. USENIX Annu. Technical Conf.*, Jun. 2010, pp. 21–34.
- [4] Y. Wen, X. Zhu, J. J. P. C. Rodrigues, and C.-W. Chen, “Cloud mobile media: Reflections and outlook,” *IEEE Trans. Multimedia*, vol. 16, no. 4, pp. 885–902, Jun. 2014.
- [5] W. Yin, J. Luo, and C.-W. Chen, “Event-based semantic image adaptation for user-centric mobile display devices,” *IEEE Trans. Multimedia*, vol. 13, no. 3, pp. 432–442, Jun. 2011.
- [6] E. Reinhard *et al.*, *High Dynamic Range Imaging: Acquisition, Display, Image-Based Lighting*, 2nd ed. San Mateo, CA, USA: Morgan Kaufmann, 2010.
- [7] T.-H. Huang, C.-T. Kao, and H. H. Chen, “Quality enhancement of procam system by radiometric compensation,” *IEEE Multimedia Signal Process. Workshop*, pp. 192–197, Sep. 2012.
- [8] M. D. Grossberg, H. Peri, S. K. Nayar, and P. N. Belhumeur, “Making one object look like another: Controlling appearance using a projector-camera system,” in *Proc. IEEE Comput. Soc. Conf. Comput. Vis. Pattern Recog.*, Jun. 2004, vol. 1, pp. I-452–I-459.
- [9] N. Massouh, S. Colonnese, F. Cuomo, T. Okoya, and T. Pivsaev, “Experimental study on luminance preprocessing for energy-aware HTTP-based mobile video streaming,” in *Proc. Eur. Workshop Vis. Inf. Process.*, Dec. 2014, pp. 1–6.
- [10] G. Ghinea and J. P. Thomas, “Quality of perception: User quality of service in multimedia presentations,” *IEEE Trans. Multimedia*, vol. 7, no. 4, pp. 786–789, Aug. 2005.
- [11] A. Iranli, W. Lee, and M. Pedram, “HVS-aware dynamic backlight scaling in TFT-LCDs,” *IEEE Trans. Very Large Scale Integr. Syst.*, vol. 14, no. 10, pp. 1103–1116, Oct. 2006.
- [12] P.-S. Tsai, C.-K. Liang, T.-H. Huang, and H. H. Chen, “Image enhancement for backlight-scaled TFT-LCD displays,” *IEEE Trans. Circuits Syst. Video Technol.*, vol. 19, no. 4, pp. 574–583, Apr. 2009.
- [13] T.-H. Huang, K.-T. Shih, S.-L. Yeh, and H. H. Chen, “Enhancement of backlight-scaled images,” *IEEE Trans. Image Process.*, vol. 22, no. 12, pp. 4587–4597, Dec. 2013.
- [14] S.-C. Pei, C.-T. Shen, and T.-Y. Lee, “Visual enhancement using constrained L0 gradient image decomposition for low backlight displays,” *IEEE Signal Process. Lett.*, vol. 19, no. 12, pp. 813–816, Dec. 2012.
- [15] M. D. Fairchild, *Color Appearance Models*, 2nd ed. Chichester, U.K.: Wiley, 2005.
- [16] T.-H. Lan and A. H. Tewfik, “A resource management strategy in wireless multimedia communications-total power saving in mobile terminals with a guaranteed QoS,” *IEEE Trans. Multimedia*, vol. 5, no. 2, pp. 267–281, Jun. 2003.
- [17] A. Lombardo, C. Panarello, and G. Sembra, “A model-assisted cross-layer design of an energy-efficient mobile video cloud,” *IEEE Trans. Multimedia*, vol. 16, no. 8, pp. 2307–2322, Dec. 2014.
- [18] Y. Wei, S. M. Bhandarkar, and S. Chandra, “A client-side statistical prediction scheme for energy aware multimedia data streaming,” *IEEE Trans. Multimedia*, vol. 8, no. 4, pp. 866–874, Aug. 2006.
- [19] R. Guruprasad and S. Dey, “Battery aware video delivery techniques using rate adaptation and base station reconfiguration,” *IEEE Trans. Multimedia*, vol. 17, no. 9, pp. 1630–1645, Sep. 2015.
- [20] K.-T. Shih and H. H. Chen, “Color enhancement based on the anchoring theory,” in *Proc. IEEE Multimedia Signal Process. Workshop*, Sep.–Oct. 2013, pp. 153–158.
- [21] T. Smith and J. Guild, “The C.I.E. colorimetric standards and their use,” *Trans. Opt. Soc.*, vol. 33, no. 3, pp. 73–134, 1931.
- [22] A. R. Robertson, “The CIE 1976 colour difference formulae,” *Color Res. Appl.*, vol. 2, pp. 7–11, 1977.
- [23] M. D. Fairchild and R. S. Berns, “Image color appearance specification through extension of CIELAB,” *Color Res. Appl.*, vol. 18, pp. 178–190, Jun. 1993.
- [24] Y. Nayatani *et al.*, “A nonlinear color appearance model using estévez-hunt-pointer primaries,” *Color Res. Appl.*, vol. 12, pp. 231–242, Oct. 1987.
- [25] Y. Nayatani *et al.*, “Color appearance model and chromatic adaptation transform,” *Color Res. Appl.*, vol. 15, pp. 210–221, Aug. 1990.
- [26] R. W. G. Hunt, “Revised colour appearance model for related and unrelated colours,” *Color Res. Appl.*, vol. 16, pp. 146–165, Jun. 1991.
- [27] N. Moroney *et al.*, “The CIECAM02 color appearance model,” in *Proc. IS&T/SID 10th Color Imaging Conf.*, Nov. 2002, pp. 23–27.
- [28] J. Morovic, *Color Gamut Mapping*. Chichester, U.K.: Wiley, 2008.
- [29] J. Morovic and M. R. Luo, “The fundamentals of gamut mapping: A survey,” *J. Imaging Sci. Technol.*, vol. 45, no. 3, pp. 283–290, 2001.
- [30] J. Morovic, P.-L. Sun, and P. Morovic, “The gamuts of input and output colour reproduction media,” in *Proc. SPIE Electron. Imaging*, Jan. 2001, pp. 114–125.
- [31] G. J. Braun and M. D. Fairchild, “Image lightness rescaling using sigmoidal contrast enhancement functions,” *J. Electron. Imaging*, vol. 8, no. 4, pp. 380–393, Oct. 1999.
- [32] H.-S. Chen and H. Kotera, “Three-dimensional gamut mapping method based on the concept of image-dependence,” in *Proc. IS&T NIP16 Conf.*, Jan. 2000, no. 1, pp. 783–786.
- [33] L. W. MacDonald, J. Morovic, and K. Xiao, “A topographic gamut compression algorithm,” *J. Imaging Sci. Technol.*, vol. 46, no. 3, pp. 228–236, Jun. 2001.
- [34] H. Zeng, “Spring-primary mapping: Combining primary adjustment and gamut mapping for pictorials and business graphics,” in *Proc. IS&T/SID 14th Color Imaging Conf.*, Nov. 2006, pp. 240–245.
- [35] S. I. Cho, S.-J. Kang, and Y. H. Kim, “Image quality-aware backlight dimming with color and detail enhancement techniques,” *J. Display Technol.*, vol. 9, no. 2, pp. 112–121, Feb. 2013.
- [36] H. Cho and O.-K. Kwon, “A backlight dimming algorithm for low power and high image quality LCD applications,” *IEEE Trans. Consum. Electron.*, vol. 55, no. 2, pp. 839–844, May 2009.

- [37] N. Tamura, N. Tsumura, and Y. Miyake, "Masking model for accurate colorimetric characterization of LCD," *J. Soc. Inf. Display*, vol. 11, no. 2, pp. 333–339, 2003.
- [38] R. S. Berns, R. J. Motta, and M. E. Gorzynski, "CRT colorimetry," *Color Res. Appl.*, vol. 18, pp. 299–314, Oct. 1993.
- [39] Y. Kwak and L. W. MacDonald, "Accurate prediction of colours on liquid crystal displays," in *Proc. IS&T/SID 9th Color Imaging Conf.*, Nov. 2001, pp. 355–359.
- [40] "Colour measurement and management in multimedia systems and equipment. Part 4: Equipment using liquid crystal display panels," Int. Electrotech. Commission, Geneva, Switzerland, Tech. Rep. IEC 61966-4, 2000.
- [41] C. Li *et al.*, "The performance of CIECAM02," in *Proc. IS&T/SID 10th Color Imaging Conf.*, Nov. 2002, pp. 28–32.
- [42] Z. Rahman, D. J. Jobson, and G. A. Woodell, "Retinex processing for automatic image enhancement," *J. Electron. Imaging*, vol. 13, no. 1, pp. 100–110, Jan. 2004.
- [43] C.-H. Lin, C.-K. Kang, and P.-C. Hsiu, "Catch your attention: Quality-retaining power saving on mobile OLED displays," in *Proc. 51st ACM/EDAC/IEEE Design Automat. Conf.*, Jun. 2014, pp. 1–6.
- [44] F. Banterle, P. Ledda, K. Debattista, and A. Chalmers, "Inverse tone mapping," in *Proc. GRAPHITE*, 2006, pp. 349–356.
- [45] T.-H. Wang *et al.*, "Pseudo-multiple-exposure-based tone fusion with local region adjustment," *IEEE Trans. Multimedia*, vol. 17, no. 4, pp. 470–484, Apr. 2015.
- [46] K.-T. Shih, H. H. Chen, and Y.-N. Liu, "Image processing system and method," U.S. patent pending.



Kuang-Tsu Shih received the B.S. degree in electrical engineering from the National Taiwan University, Taipei, Taiwan, in 2009, and is currently working toward the Ph.D. degree in communication engineering at the National Taiwan University.

His current research interests include color image processing, color science, and computational photography.



Homer H. Chen (S'83–M'86–SM'01–F'03) received the Ph.D. degree in electrical and computer engineering from the University of Illinois at Urbana-Champaign, Urbana, IL, USA, in 1986.

Since August 2003, he has been with the College of Electrical Engineering and Computer Science, National Taiwan University, Taipei, Taiwan, where he is currently an Irving T. Ho Chair Professor. Prior to that, he held various research and development management and engineering positions with U.S. companies over a period of 17 years, including AT&T Bell Labs, Holmdel, NJ, USA; Rockwell Science Center, Thousand Oaks, CA, USA; iVast, Santa Clara, CA, USA; and Digital Island, Thousand Oaks, CA, USA. He was a U.S. delegate of the ISO and ITU standards committees and contributed to the development of many new interactive multimedia technologies that are now part of the MPEG-4 and JPEG-2000 standards. His current research interests include multimedia processing and communications.

Dr. Chen was an Associate Editor of the IEEE TRANSACTIONS ON CIRCUITS AND SYSTEMS FOR VIDEO TECHNOLOGY from 2004 to 2010, the IEEE TRANSACTIONS ON IMAGE PROCESSING from 1992 to 1994, and *Pattern Recognition* from 1989 to 1999. He served as a Guest Editor for the IEEE TRANSACTIONS ON CIRCUITS AND SYSTEMS FOR VIDEO TECHNOLOGY in 1999, the IEEE TRANSACTIONS ON MULTIMEDIA in 2011, the IEEE JOURNAL OF SELECTED TOPICS IN SIGNAL PROCESSING in 2014, and Springer *Multimedia Tools and Applications* in 2015. Currently he serves on the IEEE SPS Fourier Award Committee and Fellow Reference Committee.